Intra- and Intermicellar Triplet−Triplet Annihilation of Pyrenetetrasulfonate in an AOT Reverse Micellar Solution: Relation to the Electric Percolation Transition

Yoshihiro Mori,* Hiroyuki Shinoda, Taiji Kitagawa, and Taku Nakano

Department of Pharmaceutical Sciences, Toyama Medical and Pharmaceutical University, Sugitani, Toyama 9300194, Japan

Received: February 27, 2004

Decay behaviors of triplets were investigated as a function of temperature in ternary (water/AOT/oil) and quaternary (water/AOT/cosurfactant/oil) reverse micellar solutions. The triplet species generated by the laser irradiation of tetrasodium pyrenetetrasulfonate dissolved in a reverse micelle were detected by monitoring the triplet−triplet absorption at 430 nm. The observed decay curves were analyzed with the kinetic model combining the intermicellar triplet−triplet annihilation (TTA) with the intramicellar TTA. The kinetic model for the intermicellar TTA process was proposed on the basis of the equilibrium between the monomer and dimer micelles. The obtained kinetic parameters and thermodynamic quantities are discussed in relation to electric percolation phenomena in these micellar systems. A fraction of the dimer micelles was found to be almost constant (0.27 ± 0.03) at the percolation temperature for all of the reverse micellar systems that were investigated. Furthermore, an average number of triplets per micelle and the Gibbs free energy change for dimer micelle formation seem to be closely related to the percolation threshold. These results suggest that the laser-induced transient absorption spectroscopy of a probe is a useful method for studying dynamic behavior in micellar systems.

Introduction

A microdroplet dispersed in a reverse micellar solution or a water-in-oil (w/o) microemulsion contains a small volume of a water phase (water pool) surrounded by 10 to 10^3 surfactants.[1] These droplets behave like an isolated particle on a time scale shorter than a submicro- or nanosecond,[2] but they can collide with each other and then more than two droplets aggregate and occasionally fuse to form a larger droplet. The large droplet undergoes fission easily during a relatively short period.[2] The surrounding surfactant molecules as well as the chemical species dissolved within a droplet can exchange or transfer during the aggregation process. One of the most obvious phenomena caused by these dynamic properties in the w/o microemulsion systems is the electric percolation phenomenon. On the condition that material exchange processes can be neglected, effective electric carriers such as a sodium cation and a halide anion are isolated within a water pool or bound at the interface, and then the w/o microemulsion is an insulator although the conductivity is considerably large (10^{-6}−10^{-5} S m^{-1}) in comparison with those of the absolute insulators.[3] However, when the temperature or the water content exceeds the threshold value, the electric conductivity drastically increases, and the solution changes into a good conductor with a conductivity of 10^{-1}−10^{0} S m^{-1}.[4,5] This transition is known to occur in a reversible way.

Percolation phenomena have been most extensively investigated in reverse micellar solutions consisting of water/sodium bis(2-ethylhexyl) sulfosuccinate(AOT)/oil and/or water/AOT/cosurfactant/oil. In early investigations, many efforts were devoted to elucidating the relation between the electric percolation threshold determined by electric conductivity measurements and the physical properties of the w/o microemulsion deduced from measurements of complex permittivity,[6−11] electric birefringence,[12,13] viscosity,[13−17] self-diffusion coefficients of water with pulse-gradient spin−echo NMR,[18−20] light scattering,[12,21,22] small-angle neutron scattering,[23,24] and quenching rates of fluorescence.[21,25] Two models have been proposed on the basis of these experimental results to explain the percolation phenomenon: the bicontinuous model[13,17,18,20,23,24,26] and the dynamic percolation or cluster model.[4,6,11,27,28] In the former model, electric conduction occurs through continuous open water channels formed in the oily phase at the percolation threshold. However, in the latter model, droplets dynamically aggregate to form a cluster. The electric carrier has two sources: a counterion of surfactant, for example, a Na^+ ion for AOT, and an ionic surfactant. The former can transfer from one micelle to another one through a water channel connecting these micelles (water channel-forming model).[19,25] The latter can hop from one micelle to another within the cluster (hopping model).[18] The electric conduction drastically increases when the clusters grow greatly into a percolation cluster having a fractal nature.[11] Experimental results as well as theoretical considerations[27−29] show the dynamic percolation model with the water channel-forming mechanism to be consistent in explaining the percolation phenomena in the w/o microemulsion systems consisting of AOT and a moderate amount of water. The bicontinuous model is well founded in several systems containing a high water content in which the inversion of w/o microemulsion to o/w microemulsion can occur.[23,24,26]

In the past decade, the dynamics and energetics of droplet clustering and the additive effects in percolating w/o microemulsions have attracted a great deal of attention.[22,30−40] The clustering process of droplets is extremely endothermic, but its endothermicity is nicely compensated by a great positive entropy change, leading to negative free energy.[22,30,33,34,38] As a result, the cluster formation is a rather thermodynamically favorable process. The additives can strongly affect the energies of droplet clustering.[30−32] Thus, the percolation threshold shifts largely

* Corresponding author. E-mail: moriyh@ms.toyama-mpu.ac.jp.

10.1021/jp040180p CCC: $27.50
Published on Web 09/21/2004

depending on the nature and the amount of the additive.[30−32,39,40] For example, alkanols with a long alkyl chain[22,40] and cholesterol[18,30] retard the percolation transition. However, several molecules such as poly(oxyethylene) alkyl ether (C_iE_j)[22,35−37] and sodium cholate[31,32] assist it. Alcohol molecules with a long alkyl chain can penetrate the surfactant layer of a reverse micelle and form a complex with AOT to increase the stiffness of the micellar shell.[22,41] This may cause a reduction in the attractive force that induces the fusion of the encountered droplets. The attractive force between the droplets has been suggested to be one of the parameters that determines the percolation threshold.[42] Furthermore, the oily solvent can affect droplet clustering and then percolation behavior.[32,39]

In the dynamic percolation model, the intermicellar material-exchange process plays an important role, as mentioned above. In fact, the existence of only a weakly bound cluster likely causes no electric conduction.[11] Experimental evidence for the intermicellar material exchange has been provided by fluorescence measurements involving quenching experiments,[25,38,43] excimer formation,[44] energy transfer,[45] and delayed fluorescence induced by triplet−triplet annihilation.[46] The rate constants for the intermicellar material exchange that were determined with the kinetic analysis of fluorescence quenching are found to be closely related to the percolation threshold. The percolation transition occurs when the exchange rate constants within a cluster and between clusters exceed $(1-2) \times 10^9$ $M^{-1}s^{-1}$ [21,25] and 3.8×10^8 $M^{-1}s^{-1}$,[43] respectively. These critical rate constants seem to exist irrespective of the nature of the w/o microemulsion (solvent, water content), although its physical meaning has not been made clear. Measurements of the water diffusion coefficient with PGSE NMR have also provided evidence that the material exchange of water, Na^+ ions, and surfactant molecules between droplets is closely related to the electric percolation.[19,47]

The transient absorption spectroscopy of laser- or radiation-induced transient species dissolved in a droplet seems to be as useful a method for the elucidation of intermicellar dynamics as the fluorescence methods. However, its application is limited.[48] This is mainly due to two disadvantages. The first is that the observed transient absorption (TA) spectra are very complicated because of the spectral overlap of several coexisting transients; therefore, their assignments and spectral purification are difficult. The second is that the decay mechanisms of the observed transient species have not been established. Recently, we have overcome these difficulties through systematic spectroscopic investigations of major transient species[49,50] and the final products[51] formed by the laser irradiation of several pyrene derivatives such as sodium pyrenesulfonate (NaPS) and tetrasodium 1,3,6,8-pyrenetetrasufonate (Na_4PS_4), which are well known to be fluorescent probe molecules. Cation radicals as well as triplet species generated from PS^- and PS_4^{4-} are spectroscopically separable from the other transients. The cation radical from PS^- ($P^{\bullet+}S^-$) and triplet species (T) from PS^- and PS_4^{4-} decay mainly via the following bimolecular process (eq 1) and triplet−triplet annihilation (TTA), forming different products (eqs 2 and 3; S = singlet ground state, S* = singlet excited state), respectively

$$P^{\bullet+}S^- + PS^- \rightarrow \text{products} \quad (1)$$

$$T + T \rightarrow S + S^* (PS^-) \quad (2)$$

$$T + T \rightarrow T + S (PS_4^{4-}) \quad (3)$$

When these bimolecular quenching reactions occur within a micelle or between micelles, both quenching processes (intra- and intermicellar processes) can be differentiated from each other on the basis of different rate constants. It is likely that the intramicellar quenching reaction proceeds very rapidly, whereas the intermicellar one occurs as slowly as in an aqueous solution at the dilution limit. In fact, the observed decay curves of triplet species from PS^- and PS_4^{4-} dissolved in an AOT reverse micellar solution can be successfully fit with the combined decay functions that were derived from the intra- and intermicellar TTA kinetics. As a result, both processes are clearly separable. Herein, we extend this analysis to percolation w/o microemulsion. The decay curves of triplets from PS_4^{4-} were observed as a function of temperature in AOT reverse micellar solutions with a different water content and cosurfactant. To analyze the intermicellar TTA process, we proposed a kinetic model by assuming an equilibrium between monomeric and dimeric micelles in the prepercolative region. The relations between the percolation temperature and the obtained kinetic and thermodynamic parameters are discussed.

Experimental Section

Sample Preparation. AOT (Tokyo Kasei) was purified following the method previously reported.[52] Pentaethylene glycol mono-*n*-tetradecyl ethers ($C_{14}E_5$, Nikko Chemicals), *n*-decanol (Wako Pure Chemical), and solvents (isooctane, *n*-decane; Wako Pure Chemical) that are commercially available were also used without further purification. Na_4PS_4 was purchased from Molecular Probe and used as received. Doubly distilled deionized water was employed.

Reverse micellar solutions were prepared by dissolving and mixing a constant volume of water into (AOT + cosurfactant)/isooctane or *n*-decane solution. In most of the sample solutions that were investigated, the molar concentrations of AOT ([AOT]) and Na_4PS_4 were adjusted to 0.1 and 1.0×10^{-4} M, respectively. The molar ratio of $[H_2O]/[AOT]$ ($= W$) was changed to be in the range of 55 to 40. Hereafter, we abbreviate the micellar solution with a different W value to W## solution, for example, W50. The sample solution was deaerated via several freeze−pump−thaw cycles and then displaced by Ar gas.

Measurements of Temperature-Dependent TA. The method for measuring laser-induced TA spectra and decay behavior was performed as described previously.[48] The excitation was performed with the third harmonic of a Nd:YAG laser (355 nm) unfocused at about 6 mJ/8 mm^2 and with a XeF excimer laser (351 nm) focused at about 3−4 mJ/6 mm^2. A short-arc Xe lamp was used as the monitoring light source. The effective optical cell length (L) was 0.30 ± 0.02 or 0.36 ± 0.02 for the excitation with the Nd:YAG or the XeF excimer laser, respectively. The signal at each wavelength, detected with the photomultiplier, was stored on a digital oscilloscope and transferred to a personal computer. The observed temporal range after laser irradiation was covered from 0 to 90 μs at 50 ns per point. Each signal was averaged for 10 shots of laser irradiation. The temperature of the solution was controlled using a water circulator and measured with a corrected chromel−alumel thermocouple. The accuracy of the temperature was ± 0.1 K (283−308 K) and $\leq \pm 0.2$ K (309−323 K).

Conductivity Measurements. The conductivity of the sample solution was measured as a function of temperature. The accuracy of the temperature was ± 0.1 K. The conductivity measurement was performed at 1 kHz using an LCR meter (HP4263B; Hewlet-Packard).

TABLE 1: Percolation Temperatures (T_{pr}, T_{pi}), Rate Constants (k_1, k_2) at T_{pr} and T_{pi} and Activation Energies (ΔE) for k_2 in Water/AOT (+ Cosurfactant)/Oil Reverse Micellar Solutions[a]

no.	sample solutions	T_{pr}[d] (K)	T_{pi}[d] (K)	$(k_2)_{T_{pr}}$[e] ($M^{-1}s^{-1}$)	$(k_2)_{T_{pi}}$[e] ($M^{-1}s^{-1}$)	ΔE (kJ mol^{-1})	$(k_1)_{T_{pr}}$[f] (s^{-1})
1	$C_{14}E_5$/AOT = 0.20, $W = 50$[b]	291.3	293.2	7.1×10^8	1.0×10^9	131 ± 3	1.7×10^5
2	$C_{14}E_5$/AOT = 0.15, $W = 50$[b]	297.6	300.2	7.0×10^8	1.2×10^9	148 ± 4	1.6×10^5
3	$C_{14}E_5$/AOT=0.10, $W = 50$[b]	306.7	309.0	8.1×10^8	1.3×10^9	162 ± 5	1.7×10^5
4	*n*-decanol/AOT = 0.15, $W = 50$[b]	315.0	317.2	1.2×10^9	2.0×10^9	189 ± 6	2.0×10^5
5	W=50 (0.1 M AOT/isooctane)[b]	308.6	309.7	7.9×10^8	1.0×10^9	176 ± 8	1.7×10^5
5′	$W = 50$ (0.1 M AOT/isooctane)[c]	308.4	309.7	5.6×10^8	7.0×10^8	176 ± 8	1.8×10^5
6	$W = 55$ (0.1 M AOT/isooctane)[c]	305.3	306.2	5.4×10^8	6.8×10^8	200 ± 6	1.7×10^5
7	$W = 45$ (0.1 M AOT/isooctane)[c]	313.0	314.6	6.3×10^8	8.5×10^8	151 ± 9	2.0×10^5
8	W40 (0.18MAOT/*n*-decane)[c]	297.1	298.7	3.0×10^8	4.7×10^8	196 ± 6	2.2×10^5
9	W30 (0.18MAOT/*n*-decane)[c]	[g]	306.5		7.4×10^8	140 ± 2	
10	W26 (0.18MAOT/*n*-decane)[c]	[g]	310.3		8.3×10^8	117 ± 3	

[a] The errors presented are standard deviations. [b] 0.1M AOT/isooctane solution, excitation laser: Nd:YAG laser (355 nm). [c] Excitation laser: XeF laser (351 nm). [d] The estimated errors are within ±0.2 to ±0.3 K for all data. [e] The rate constants of k_2 at T_{pr} and T_{pi} were estimated by interpolation on the Arrhenius plot calculated with the least-squares fitting method. [f] The rate constants of k_1 at T_{pi} were graphically estimated. [g] T_{pr} of these solutions could not be determined because the rising gradients in their conductivity vs temperature curves were much smaller than that of sample solution no. 8.

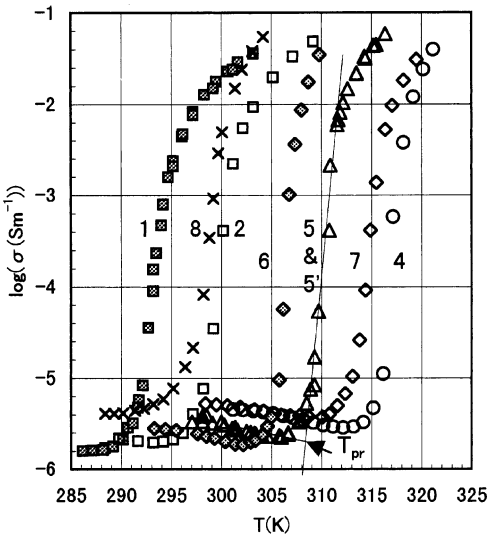

Figure 1. Temperature dependence of electric conductivity measured in the reverse micellar solutions consisting of water/AOT, cosurfactant/isooctane, or decane. The attached numbers 1, 2, and 4−8 correspond to the number of the sample solution given in Table 1. The percolation temperature T_{pr} for sample solution no. 5 was determined from the crossing point of the two linear curves calculated by the least-squares fitting method.

Results

Determination of Percolation Temperatures. Figure 1 shows the temperature dependence of electric conductivity observed in several reverse micellar solutions. We determined two types of percolation temperatures, T_{pr} and T_{pi}, by analyzing the observed electric conductivity versus temperature curves. T_{pr} is the temperature of the onset of the percolation transition. This temperature was estimated with the least-squares fitting method. An example of the W50 solution is illustrated in Figure 1. T_{pi} is the temperature at the inflection point appearing in the conductivity versus temperature curve above T_{pr}. The two percolation temperatures, T_{pr} and T_{pi}, were determined to be 308.6 ± 0.2 and 309.7 ± 0.3 K, respectively, for the W50 solution. The results are summarized in Table 1. The observed percolation temperatures in this work are consistent with the previous data available.[21,22,25,32,35,38−40]

Analysis of Decay Curves for T−T Absorption. The T−T absorption peak of the PS_4^{4-} ion was observed at 430 nm both in aqueous and reverse micellar solutions. The detailed analytical procedures for the triplet decay curve that was observed at this peak were described previously.[50] Here, we summarize them briefly. The contamination due to the cation radical, one of the most dominant transient species other than the triplet, was negligibly small at 430 nm.[50] Small but significant contamination was detected from the hot $(PS_4^{4-})^{\ddagger}$.[50] This transient has a lifetime of about 1.5 ms. Therefore, this contamination can be eliminated by selecting the temporal range for the analysis where the contribution from the $(PS_4^{4-})^{\ddagger}$ is negligibly small, that is, $t > 1.5\ \mu s$. The elimination of this contaminant can also be carried out in a strict way.[50] Thus, the decay curve purely due to T−T absorption is separable from the observed ones. In addition, the molar extinction coefficient of the T−T absorption at this wavelength (17 000 ± 1000 M^{-1} cm^{-1}) is independent of whether the probe molecule is placed in a reverse micelle or a bulk aqueous solution.[49,50]

The triplets generated in the reverse micellar solutions decay via the following two processes:

i. Intramicellar TTA Process. Within micelles containing more than two triplets, the intramicellar TTA process proceeds rapidly obeying eq 3, and finally one triplet remains in each micelle. The rate, eq 4, for this process can be derived by assuming a Poisson distribution for the initial population of triplets per micelle.[50,53]

$$A(t) = -\left(\frac{2A(0)}{T_{av}}\right)\sum a_j \exp[-0.5\, k_1 j\,(j-1)t] \qquad (4)$$

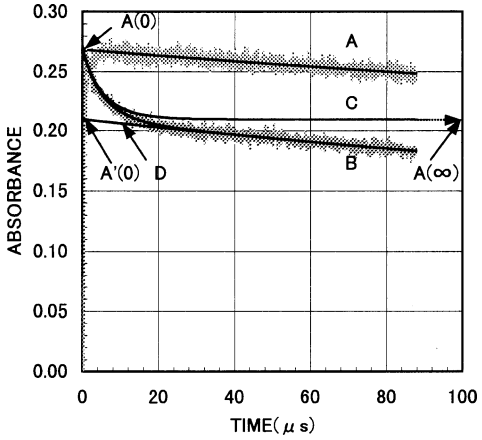

Figure 2. Kinetic analysis of the decay curve of T−T absorption based on the intra- and intermicellar TTA mechanisms. The decay curves observed in aqueous solution (upper) and W50 solution (lower; no. 5′ in Table 1) were analyzed. The contribution from a minor contaminant $(PS_4^{4-})^{\ddagger}$ was corrected by subtracting the following exponential decay function: $0.04 \exp(-t/\tau)$ ($\tau = 1.5$ ms). The definitions of four calculated curves, A−D, and three characteristic absorbance values, $A(0)$, $A'(0)$, and $A(\infty)$, are described in the text.

where $A(t)$ and $A(0)$ are the absorbances at $t = t$ and 0, respectively, that are observed in the reverse micellar solution. In eq 4, T_{av} is the average triplet number per micelle and k_1 is the rate constant (s^{-1}) for the TTA of a pair of triplets in a micelle obeying eq 3. The coefficient a_j is a complicated function of j (1−∞) involving T_{av}, where j is the number of triplets in a micelle. From eq 4, the absorbance at $t = \infty$, $A(\infty)$, is given by eq 5.

$$A(\infty) = A(0)\frac{1 - \exp(-T_{av})}{T_{av}} \tag{5}$$

T_{av} can be calculated from eq 5 when $A(0)$ and $A(\infty)$ are known.

ii. Intermicellar TTA Process. The surviving triplets after the completion of the intramicellar TTA, of which concentration is proportional to $A(\infty)$, further decay via the intermicellar TTA process. The rate equation for this process can be described by a bimolecular rate equation, that is,

$$A(t) = \frac{A'(0)}{1 + A'(0)\left(\frac{k_2}{\epsilon L}\right)t} \tag{6}$$

where ϵ and L are the molar extinction coefficient and the effective optical path length, respectively.

The fitting analysis was carried out using the two-step procedures. The results are shown as an example in Figure 2. In the first step, the observed decay curve was fit to eq 6 in the temporal range where the contribution of the intramicellar TTA was negligibly small ($t >$ 10−20 μs). In this procedure, we obtained two parameters: k_2 and $A'(0)$. Curve D in Figure 2 shows the fitting curve. T_{av} was estimated from eq 5 with $A(\infty)$ and $A(0)$, where we used the following two relations: $A(\infty) = A'(0)$ and $A(0) = A_{aq}(0)$. $A_{aq}(0)$ was obtained by fitting the corresponding decay curve in aqueous solution to eq 6 (curve A in Figure 2). In the second step, the residual decay curve after subtracting the contribution of the intermicellar TTA (curve D) was fit to eq 4, leading to the determination of k_1. Curves C and B in Figure 2 show the fitting curves due to the intramicellar and the overall TTA processes, respectively. The two-step fitting analysis was assessed by comparing the micellar concentration that was estimated from T_{av} and the triplet concentration

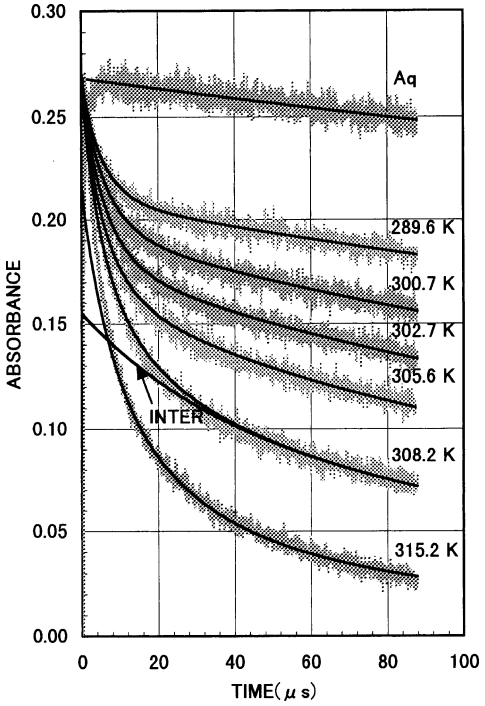

Figure 3. Temperature-dependent decay curves for the T−T absorption observed in the W50 solution (sample solution no. 5′ in Table 1) and their fitting curves (shown as bald curves). The calculated curves below 308.2 K present the sum of the contributions from the intra- and intermicellar TTA processes. Two calculated curves at 315.2 and 308.2 K (curve "INTER") show only the contribution from the intermicellar TTA.

($= A(0)/\epsilon L$) with the literature values available. As a result, both micellar concentrations agreed well. For example, the average micellar concentration in the W50 solution containing no cosurfactant at 293−298 K was $(7.2 \pm 0.9) \times 10^{-5}$ mol dm^{-3}, in agreement with the literature value (7.3×10^{-5} mol dm^{-3}).[54]

Figure 3shows a marked temperature dependence of the triplet decay curves in the W50 micellar solutions. The fitting curves given by bald curves excellently reproduced the observed decay curves in the temperature range below T_{pi} (= 308.4 K). Similar temperature-dependent decay curves were also observed in the reverse micellar solutions with different compositions and solvents as listed in Table 1. The rate constants for the intra- and intermicellar TTA processes, k_1 and k_2, and T_{av} were obtained as a function of temperature. Six tentative results are shown in Figure 4. In any system, the values of k_2 are found to increase monotonically with the increase in temperature. It is shown in Figure 4 that T_{av} attains the maximum value near the percolation temperatures and then decreases. The increase in T_{av} toward T_{pr} indicates that the micellar concentration decreases with the increase in temperature; that is, the size of the water pool becomes large. This enlargement is consistent with the fact that k_1 slightly decreases with the increase in temperature below T_{pr}. However, the decrease in T_{av} above T_{pr} seems to be due to the very rapid intermicellar TTA process in the percolation domain, leading to the apparently large value of $A'(0)$ in eq 6. This means that the kinetic model used in this analysis is unsuitable; that is, the intra- and intermicellar TTA processes are not separable from each other. In fact, in the temperature range far above T_{pi} (postpercolation domain), the decay curves can be fit excellently with the intermicellar TTA model presented by eq 6 without any contribution from the intramicellar TTA process. Figure 5 shows a tentative example.

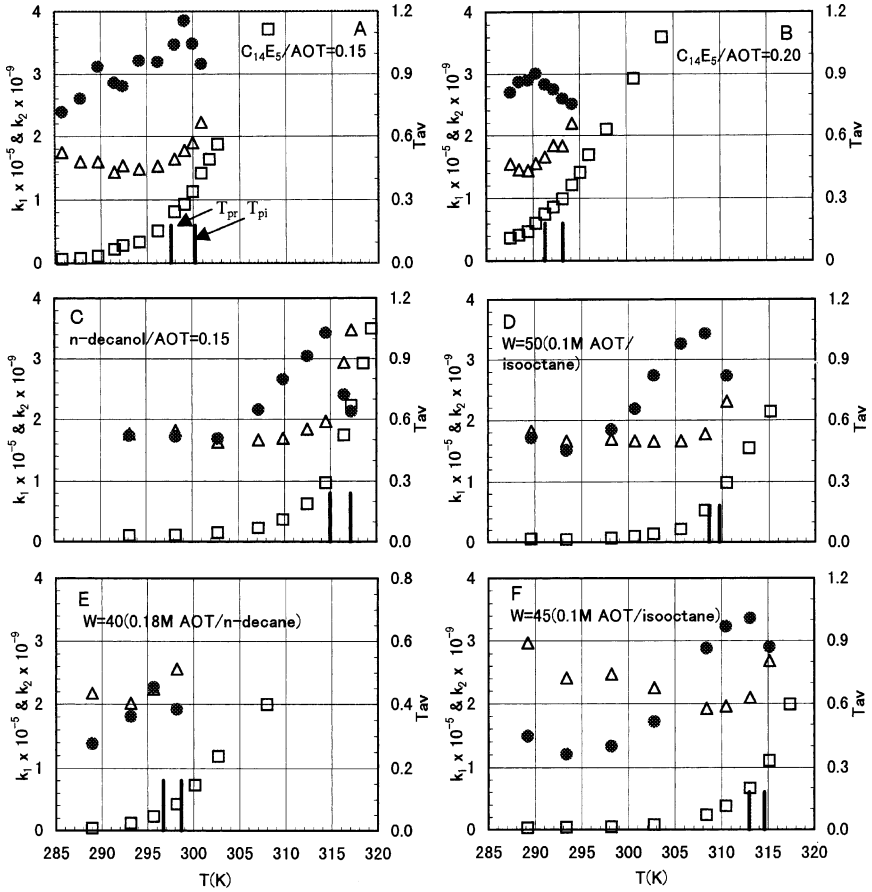

Figure 4. Temperature dependence of k_1 (△), k_2 (□), and T_{av} (●) in six reverse micellar solutions with different compositions. A−F correspond to the sample solutions of no. 2, 1, 4, 5′, 8, and 7, respectively. Two short bars present the percolation temperatures T_{pr} (left) and T_{pi} (right).

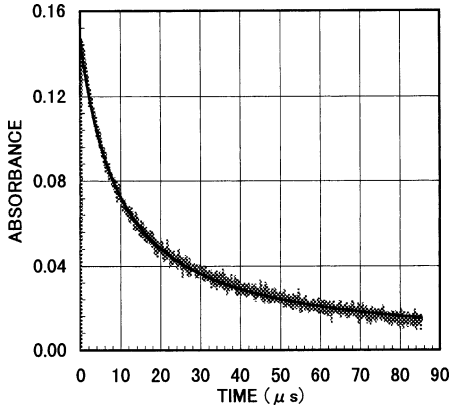

Figure 5. Observed and fitting curves of T−T absorption in the postpercolation domain (303.8 K, sample solution no. 1 ($C_{14}E_5$/AOT = 0.20)). The bald curve was calculated by fitting the observed curve to eq 6 with the least-squares fitting method. Rate constant k_2 was determined to be $(3.6 \pm 0.4) \times 10^9$ M^{-1} s^{-1}.

Cluster Model or Bicontinuous Model? The monotonic increase in k_2 in the temperature range up to far above T_{pi} as shown in Figure 4 provides clear evidence that TTA and then electric percolation never occur within a bicontinuous water channel in all of the reverse micellar solutions that were investigated. If the bicontinuous phase is formed in the percolation state, then rate constant k_2 is likely to attain the maximum value expected at the maximum triplet concentration of in the water channel. This concentration is roughly estimated to be proportional to the concentration of probes dissolved into the total amount of water solubilized in a reverse micellar solution. For example, the concentration is equal to about 4×10^{-4} M for the W50 solution including 0.1 M AOT and 1×10^{-4} M probe molecules when the triplet yield is 0.4.[49] This is much less than the apparent triplet concentration in the water pool containing two triplets (1.6×10^{-3} M) where the TTA rate constants (k_1) are in the range of $(1.6-2.0) \times 10^5$ s^{-1}, corresponding to $(1.0-1.3) \times 10^8$ M^{-1} s^{-1} for the bimolecular rate constant. This value is in agreement with the bimolecular TTA rate constants that were measured in aqueous solution ($(1.0 \pm 0.3) \times 10^8$ M^{-1} s^{-1}).[55] Therefore, the observed large rate constants of k_2 ($\leq 1 \times 10^{10}$ M^{-1} s^{-1}) at far above T_{pi} can never be explained by the bicontinuous model. To understand such an apparent bimolecular and very rapid TTA process, we consider the cluster model to be an alternative model for the electric percolation mechanism. In the cluster model, N micelles are dynamically aggregated and fused to generate a large micelle that encloses a water pool with a volume of NV_0 (V_0 = volume of water pool before fusion) containing M triplets. The TTA rate within a fused cluster is considered to be comparable with the intramicellar TTA rate because the apparent triplet concentration in a fused cluster ($M/(NV_0)$) is nearly equal to T_{av}/V_0. When the cluster formation rate is comparable with or faster than the intracluster TTA rate, the concept of intercluster or intermicellar TTA becomes very vague. In other words, triplet species could be supplied from different micelles or clusters during the intracluster TTA. In the limiting case, the triplet decay curves could be described only by the intracluster TTA process, of which the kinetic equation may be approximately presented by eq 6. Thus, the cluster model is consistent with the observed temperature-dependent T−T absorption data.

Kinetic Model for the Intermicellar TTA Process. We propose the intradimer TTA model to analyze the kinetic data

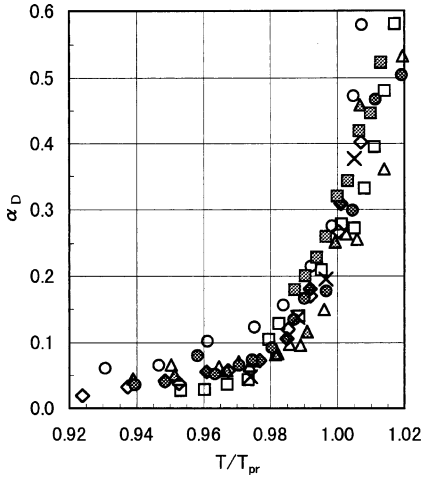

Figure 6. Relation between α_D and the reduced temperature (T/T_{pr}). The data were obtained by analyzing the temperature-dependent decay curves of T−T absorption in nine reverse micellar solutions as listed in Table 1: 1 (■), 2 (□), 3 (●), 4 (○), 5 (△), 5′ (▲), 6 (◇), 7 (♦), and 8 (×).

SCHEME 1 Reaction Mechanism of Intermicellar TTA

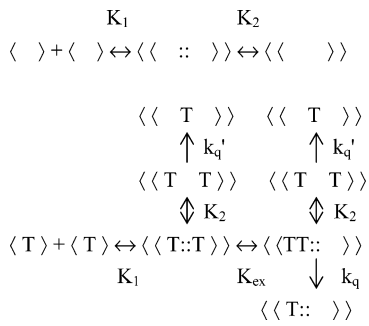

that was obtained in the prepercolation states ($T \leq T_{pi}$) where the existence of a large fused cluster can be neglected. The basic idea is due to the well-known fusion and fission mechanisms of the micellar droplets. The reaction pathway shown in Scheme 1 was considered. In this scheme, ⟨T⟩ and ⟨ ⟩ show the monomer micelles that contain one triplet and no triplet, respectively. The three symbols ⟨⟨T::T⟩⟩, ⟨⟨TT:: ⟩⟩, and ⟨⟨ :: ⟩⟩ indicate the partially fused-dimer micelles, of which water pools are connected through a narrow water channel, illustrated as double colons, "::". The triplets can quickly transfer thorough this channel, leading to the formation of ⟨⟨TT:: ⟩⟩, where two triplets eventually accumulate in either compartment. The completely fused-dimer micelles with a doubly expanded water pool are denoted with symbols such as ⟨⟨TT⟩⟩ and ⟨⟨ ⟩⟩. The effective quenching of the triplets that are trapped within a micelle occurs only within ⟨⟨TT:: ⟩⟩ and ⟨⟨TT⟩⟩. Therefore, the rate equation for the intermicellar TTA process is given by eq 7a.

$$\frac{d[T]}{dt} = -k_q[\langle\langle TT::\rangle\rangle] - k_q'[\langle\langle TT\rangle\rangle] \quad (7a)$$

$$= -\left(\frac{1}{2}\right)k_q[\langle\langle T::T\rangle\rangle + \langle\langle TT::\rangle\rangle + \langle\langle TT\rangle\rangle] \quad (7b)$$

$$= -\left(\frac{1}{2}\right)k_q\frac{\alpha_D}{[M + D]}[T]^2 \quad (7c)$$

In the transformation from eq 7a to eq 7b, the following assumptions were used:

(1) The exchange of triplets through the water channel in a partially fused-dimer micelle occurs very rapidly, leading to the following relation: $[\langle\langle T::T\rangle\rangle] = [\langle\langle TT::\rangle\rangle]$

TABLE 2: α_D at T_{pr} and the Thermodynamic Quantities (ΔH, ΔS, and ΔG_{md} at T_{pr}) for the Equilibrium between the Monomer and Dimer Micelles in Water/AOT (+ Cosurfactant)/Oil Reverse Micellar Solutions[a]

no.[b]	$(\alpha_D)_{T_{pr}}$	ΔH (kJ mol^{-1})	ΔS (J K^{-1})	$(\Delta G_{md})_{T_{pr}}$ (kJ mol^{-1})
1	0.32	185 ± 6	717 ± 19	−23.8
2	0.27	180 ± 7	686 ± 25	−24.2
3	0.25	181 ± 9	671 ± 28	−24.8
4	0.30	211 ± 19	753 ± 61	−26.2
5	0.28	186 ± 11	683 ± 40	−24.8
5′	0.22	189 ± 23	689 ± 77	−23.5
6	0.28	241 ± 10	867 ± 33	−23.7
7	0.27	181 ± 13	657 ± 41	−24.6
8	0.27	253 ± 9	924 ± 32	−21.2
av	0.27 ± 0.03			−24.1 ± 1.3

[a] The errors presented are standard deviations. [b] Numbers 1−8 correspond to the sample solutions in Table 1.

(2) The volume of the water pool in a completely fused-dimer micelle is assumed to be twice that of the monomer micelle. This leads to the relation $k_q' = k_q/2$.

Furthermore, eq 7c was derived on the basis of eqs 8−10

$$\frac{[\langle\langle T::T\rangle\rangle + \langle\langle TT::\rangle\rangle + \langle\langle TT\rangle\rangle]}{[\langle T\rangle]^2} = \frac{[D]}{[M]^2} = K \quad (8)$$

where [D] (= $[\langle\langle :: \rangle\rangle]$ + $[\langle\langle \rangle\rangle]$) and [M] (= $[\langle \rangle]$) are the concentrations of dimer and monomer micelles, respectively.

$$[\langle T\rangle] = \left\{\frac{[M]}{([M] + [D])}\right\}[T] \quad (9)$$

$$\alpha_D = \frac{[D]}{([M] + [D])} \quad (10)$$

Thus, the apparent rate constant k_2 for the intermicellar TTA, determined experimentally from eq 6, is given by

$$k_2 = \left(\frac{1}{2}\right)k_q\frac{\alpha_D}{[M] + [D]} \quad (11)$$

In eq 11 we can reasonably assume that $k_q = k_1$. The micellar concentration of ([M] + [D]) can be estimated from the relation $[T]_0/([M] + [D]) = T_{av}$, where $[T]_0 = A(0)/(\epsilon L)$. Thus, α_D can be estimated from k_2, leading to the determination of the equilibrium constants (K) for the monomer ([M])−fused dimer ([D]) equilibrium, that is, $K = K_1 + K_1K_2$.

Figure 6 shows the relation between α_D and the scaled temperature, T/T_{pr}. It is found that α_D is nearly constant (0.27 ± 0.03) at the percolation temperature T_{pr} in all of the reverse micellar systems that were investigated. The results are summarized in Table 2.

Thermodynamic Quantities. Figure 7 shows the Arrhenius plots for k_2. It is found that the Arrhenius plots significantly deviate in the temperature ranges above T_{pi} as well as those far below T_{pr}. The former deviation suggests that the assumption for the equilibrium between the monomer and dimer micelles may be incorrect in the postpercolation state. The latter is likely due to the dominant contribution other than the intermicellar TTA process, for example, the spontaneous decay of the triplet in the micellar environment. The obtained activation energies (ΔE), summarized in Table 1, are very large (>100 kJ mol^{-1}) for all of the reverse micellar solutions that were investigated. This suggests that the intermicellar TTA process is markedly

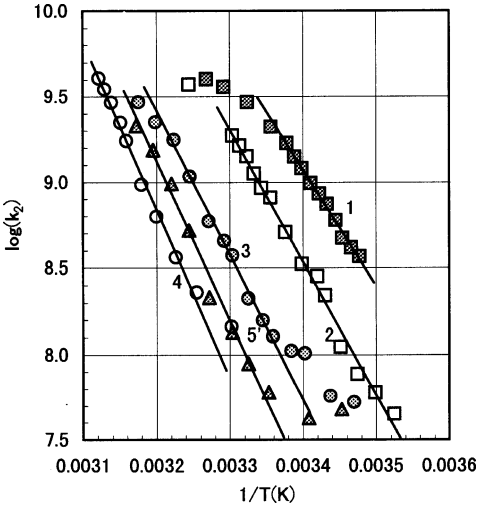

Figure 7. Arrhenius plots for k_2 in five selected reverse micellar solutions. Solid lines show the least-squares fitting lines. The attached numbers correspond to the sample solutions given in Table 1: 1 (■), 2 (□), 3 (●), 4 (○), and 5′ (▲).

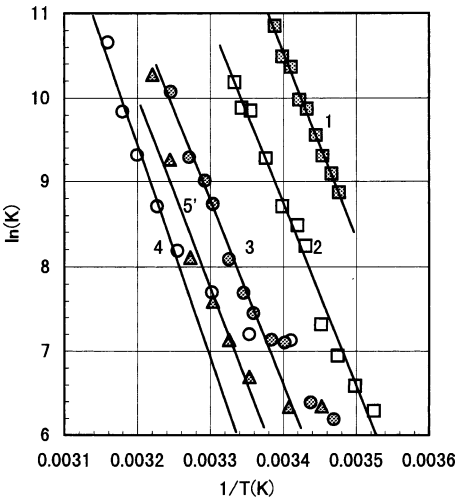

Figure 8. van't Hoff plots for the equilibrium constants (K) between the monomer and fused-dimer micelles. The solid curves show the least-squares fitting lines. The numbers and symbols are the same as those given in Figure 7.

endothermic. Such a large activation energy and similar W dependency were previously reported in the activation energies of the intercluster material exchange process.[2,38]

Figure 8 shows the van't Hoff plots for the equilibrium constants (K) between the monomer and dimer micelles obtained from α_D and [M] + [D]. The least-squares fitting was carried out for the data that was obtained in the temperature range below T_{pi} and above the temperature where the spontaneous decay was neglected. The obtained enthalpy (ΔH) and entropy changes (ΔS) and the calculated Gibbs free energy changes at T_{pr} (ΔG_{md}) are given in Table 2. These thermodynamic quantities can be compared with the literature values obtained in W25 and W35 water/AOT/isooctane solutions.[9,16,34] Our data (ΔH) obtained in W45−W55 solutions are much larger by 60 (W45)−120 (W55) kJ mol^{-1} than the literature values for the W35 solution, that is, 119 ±1[9] and 121[16] kJ mol^{-1}. This difference may be explained by the W dependence of ΔH.[9] The values of ΔH and ΔS seem to be larger than the droplet-clustering enthalpy and entropy in several AOT-stabilized w/o microemulsion systems reported previously.[22,30−34,40]

Discussion

On the basis of the proposed kinetic model for the TTA process in a reverse micellar solution, we obtained two rate constants, k_1 and k_2, for the intra- and intermicellar TTA, respectively. These rate constants were successfully determined only when the intramicellar TTA process was separable from the intermicellar one, that is, in the prepercolation region. Furthermore, the intermicellar TTA process was analyzed by assuming that the monomer and the fused-dimer micelles were in equilibrium, leading us to determine the fraction of dimer micelle (α_D) as well as the thermodynamic quantities related to the monomer−dimer micelle equilibrium. Herein, we discuss the results from two points of view.

First, we briefly review the results from the luminescence quenching experiments reported previously in comparison with our kinetic model for the TTA. It is well known that the luminescence quenching in a micellar solution can be described by the nonlinear Infelta−Tachiya equation.[56,57] This equation was extended to a reverse micellar solution by Jóhannsson and Almgren[58,59] and Mays,[38,43] and it involves four rate constants: the natural decay constant and the intramicellar, intracluster, and intercluster quenching constants. All four rate constants are required as parameters when the luminescence lifetime of the probe molecule used is as long as a few milliseconds. However, the two former constants are enough to describe the luminescence decay curves when the lifetime is very short, on the order of nanoseconds; that is, the luminescence decays dominantly via the intramicellar quenching process. The extended Infelta−Tachiya equation also involves the size of a cluster (N_c) as one of the fitting parameters, defined by the average aggregation number of micelles per cluster. The parameter N_c can be estimated from an initial drop of the observed luminescence decay curve under the limited experimental conditions.[38,58] In most cases investigated experimentally, however, the cluster characteristics (size, shape, distribution, etc.) seem to remain indefinite.[38,43,59] This may be due to the fact that a cluster appears as a highly dynamic aggregate.[2,34,38] Nevertheless, a fused-dimer micelle formed from two micelles is often proposed to be an effective intermediate where the luminescent probe molecule and a quencher can easily exchange and interact with each other. The additional micelles weakly bound to the fused dimer may act as a heat or a surfactant reservoir in the fusion−fission process. Their roles, however, have not been explicitly evaluated in the kinetic analysis. In our monomer−dimer model for the TTA analysis, these additional weakly bound micelles, even if they were present, are assumed to behave like free-monomer micelles. This assumption is considered to be valid in the prepercolation state where N_c is small[58] and the encounter micelles formed via nonsticky collision disintegrate in a period much shorter than the lifetime of the fused dimer.[2] It is unlikely that a fused micelle larger than the dimer is formed in this state. At temperatures above the percolation transition ($T > T_{pi}$), however, clusters grow, and multiple fused clusters such as the dimer and the trimer are formed in a transient way. Thus, the intercluster quenching dominantly occurs, and then luminescence decay profile is a single exponential.[43] The intermicellar TTA rates also greatly increase in this temperature region and are comparable with those for the intramicellar TTA. As a result, the observed triplet decay curves were described by simple secondary reaction kinetics (eq 6). In the intermediate state, that is, the transition temperature region around T_{pi}, a significant number of completely fused dimers ($\langle\langle\ \rangle\rangle$) likely coexist in the micellar solutions investigated because $\alpha_D > 0.3$, as shown in Figure 6. This may cause the polydispersity of rate constants

k_1 and, consequently, k_2. Therefore, both of the rate constants obtained at temperatures around T_{pi} should be regarded as "average values" reflecting the polydispersity of the corresponding micellar solution.

Second, we discuss the relations between the percolation temperature and the following four parameters that were determined from the kinetic analysis of TTA: ΔE, T_{av}, α_D, and ΔG_{md}.

ΔE. When $C_{14}E_5$ was added as a cosurfactant, T_{pi} decreased with the increase in the amount added, whereas the opposite shift was observed when *n*-decanol was added. This result can be explained on the basis of the nature of the two cosurfactants: $C_{14}E_5$ is one of the cosurfactants that can enhance the fluidity of the micellar interface ("softener"),[22] and inversely, *n*-decanol works as a "hardener".[22,41] The activation energies for k_2 (ΔEs) that were obtained in the quaternary reverse micellar systems (sample solutions nos. 1−4 in Table 1) reflect these properties of the two cosurfactants: The softener ($C_{14}E_5$) lowers the activation energy together with the percolation temperature, whereas the hardener (*n*-decanol) enhances both of them. The T_{pi} (or T_{pr}) data given in Table 1 show that the percolation temperatures decrease with the increase in *W*. However ΔEs are found to increase markedly with the increase in *W* (sample solutions nos. 5−10 in Table 1). Such an antipodal relation between ΔE and the percolation temperature suggests that the change in ΔE does not necessarily decide the direction of the shift of percolation temperature. The change of fluidity in the micellar interface induced by adding a cosurfactant or chemical species seems to affect sensitively the value of ΔE.

T_{av}. The second parameter T_{av} was found to attain the maximum value near the percolation temperature. This existence of the maximum, however, should be examined carefully because the method for computing T_{av} from eq 5 is based on the assumption that the intra- and intermicellar TTA processes are separable from each other, leading to the relation $A(\infty) = A'(0)$. Therefore, the values of T_{av} determined from eq 5 under the condition where this assumption is not realized are misleading. For example, when the rate of intermicellar TTA increases to become comparable with that of the intramicellar TTA, $A'(0)$ is significantly larger than $A(\infty)$, which can be predicted by eq 4 from the initial triplet distribution. $A(\infty)$ is then overestimated if we assume the relation $A(\infty) = A'(0)$. If this is the case, then T_{av} apparently decreases above the percolation temperature. Nevertheless, the temperature presenting the apparent maximum value of T_{av} is characteristic because the intra- and intermicellar TTA processes become inseparable around this temperature. This means that percolation is initiated above this temperature.

α_D. The temperature-induced percolation transition occurs when α_D exceeds the threshold value (0.27 ± 0.03) in the reverse micellar solutions that were investigated. The threshold value is likely to be independent of the nature of the reverse micelle,that is, micellar size and hardness of the surfactant shell and solvent. The physical inherency of this constant, however, has not been fully evidenced over a wide range of reverse micellar systems, for example, with surfactants other than AOT or different solvents. Nevertheless, this finding is consistent with the cluster model that was proposed for the percolation transition. When the fraction of the dimer micelle (α_D) exceeds $^1/_4$, higher-order fusion processes are likely to occur with a significantly large probability, leading to the formation of a large cluster.

ΔG_{md}. The fourth relation is presented as follows: the Gibbs free energy for the monomer−dimer micelle equilibrium (ΔG_{md}) is nearly constant (-24.1 ± 1.3 kJ mol^{-1}) at the percolation temperature (T_{pr}). This value is comparable with the Gibbs free energies (ΔG_{cl}) of the clustering of droplets obtained in several w/o microemulsion systems. ΔG_{cl} was calculated from eq 12.[30]

$$\Delta G_{cl} = RT \ln(X_d) \tag{12}$$

where X_d is the mole fraction of a droplet at the percolation threshold.

The values of ΔG_{cl} that are reported in the literature are distributed in the range of -20 to -30 kJ mol^{-1}, depending on *W*, the additive, and the solvent.[22,30−34] The standard deviation of ΔG_{md} was much smaller than the variation range of ΔG_{cl}. Nevertheless, ΔG_{md} may involve some systematic deviation. For example, the largest deviation of ΔG_{md} that was observed in sample solution no. 8 in Table 2 may be due to the different solvent that was used. Such a systematic change for ΔG_{md} will be elucidated on the basis of the accumulated data. Then, ΔG_{md} might appear to be a good parameter for understanding the percolation phenomena because ΔG_{md} is a thermodynamic quantity that provides information on the free-energy difference between the nonpercolative micellar state and the percolation state.

Conclusions

In this work, we employed the transient absorption spectroscopy of laser-induced transient species, particularly of triplet species, to investigate the percolation phenomena in the AOT-containing reverse micellar systems. This method provides valuable information about the intra- and intermicellar dynamics of the triplet species, leading to several important relations between the percolation threshold and the micellar clustering processes: (1) The cluster model can consistently explain the observed percolation phenomena in these reverse micellar systems. (2) The percolation occurs when the mole fraction of the fused-dimer micelle exceeds the threshold value. (3) The average number of triplets per micelle apparently attains the maximum value around the percolation threshold. (4) The Gibbs free energy for the monomer−dimer micelle equilibrium seems to be nearly constant at the percolation temperature.

Acknowledgment. We thank M. Takanami, N. Shiki, T. Ikubo, and M. Kobayashi for their assistance in the preliminary measurements of TA spectra and the analysis of the decay kinetics.

References and Notes

(1) Fendler, J. H. *Membrane Mimetic Chemistry*; Wiley Interscience: New York, 1982; Chapter 1.
(2) Fletcher, P. D. I.; Howe, A. M.; Robinson, B. H. *J. Chem. Soc., Faraday Trans. 1* **1987**, *83*, 985.
(3) Eicke, H. F.; Borkovec, M.; Das-Gupta, B. *J. Phys. Chem.* **1989**, *93*, 314.
(4) Laguës, M. *J. Phys., Lett.* **1979**, *40*, L331.
(5) Laguës, M.; Sauterey, C. *J. Phys. Chem.* **1980**, *84*, 3503.
(6) Bhattacharya, S.; Stokes, J. P.; Kim, M. W.; Huang, J. S. *Phys. Rev. Lett.* **1985**, *55*, 1884.
(7) Eicke, H. F.; Geiger, S.; Sauer, F. A.; Thomas, H. *Ber. Bunsen-Ges. Phys. Chem.* **1986**, *90*, 872.
(8) van Dijk, M. A.; Casteleijn, G.; Joosten, J. G. H.; Levine, Y. K. *J. Chem. Phys.* **1986**, *85*, 626.
(9) van Dijk, M. A.; Joosten, J. G. H.; Levine, Y. K.; Bedeaux, D. *J. Phys. Chem.* **1989**, *93*, 2506.
(10) Ponton, A.; Bose, T. K.; Delbos, G. *J. Chem. Phys.* **1991**, *94*, 6879.
(11) Feldman, T.; Kozlovich, N.; Nir, I.; Garti, N. *Colloids Surf., A* **1997**, *128*, 47.
(12) Hilfiker, R.; Eicke, H. F. *J. Chem. Soc., Faraday Trans. 1* **1987**, *83*, 1621.

(13) Borkovee, B.; Eicke, H. F.; Hammerich, H.; Gupta, B. D. *J. Phys. Chem.* **1988**, *92*, 206.
(14) Eicke, H. F.; Kubik, R.; Hammerlich, H. *J. Colloid Interface Sci.* **1982**, *90*, 27.
(15) Berg, R. F.; Moldover, M. R.; Huang, J. S. *J. Chem. Phys.* **1987**, *87*, 3687.
(16) Smeets, J.; Koper, G. J. M.; van der Ploeg, J. P. M.; Bedeaux, D. *Langmuir* **1994**, *10*, 1387.
(17) Meier, W. *Colloids Surf., A* **1995**, *94*, 111.
(18) Maitra, A.; Mathew, C.; Varshney, M. *J. Phys. Chem.* **1990**, *94*, 5290.
(19) Feldman, Y.; Kozlovich, N.; Nir, I.; Garti, N.; Archipov, V.; Idiyatullin, Z.; Zuev, Y.; Fedotov, V. *J. Phys. Chem.* **1996**, *100*, 3745.
(20) Antalek, B.; Williams, A. J.; Texter, J.; Feldman, Y.; Garti, N. *Colloids Surf., A* **1997**, *128*, 1.
(21) Lang, J.; Lalem, N.; Zana, R. *Colloids Surf.* **1992**, *68*, 199.
(22) Nazário, L. M. M.; Hatton, T. A.; Crespo, J. P. S. G. *Langmuir* **1996**, *12*, 6326.
(23) Chen, S. H.; Chang, S. L.; Strey, R. *J. Chem. Phys.* **1990**, *93*, 1907.
(24) Chen, S. H.; Chang, S. L.; Strey, R.; Samseth, J.; Mortensen, K. *J. Phys. Chem.* **1991**, *95*, 7427.
(25) Jada, A.; Lang, J.; Zana, R. *J. Phys. Chem.* **1989**, *93*, 10.
(26) De Gennes, P. G.; Taupin, C. *J. Phys. Chem.* **1982**, *86*, 2294.
(27) Geiger, S.; Eicke, H. F.; Spielmann, D. *Z. Phys. B.: Condens. Matter* **1987**, *68*, 175.
(28) Cametti, C.; Codastefano, P.; Tartaglia, P.; Rouch, J.; Chen, S. H. *Phys. Rev. Lett.* **1990**, *64*, 1461.
(29) Ku, C. Y.; Chen, S. H.; Rouch, J.; Tartaglia, P. *Int. J. Thermophys.* **1995**, *16*, 1119.
(30) Ray, S.; Bisal, S. R.; Moulik, S. P. *J. Chem. Soc., Faraday Trans.* **1993**, *89*, 3277.
(31) Moulik, S. P.; De, G. C.; Bhowmik, B. B.; Panda, A. K. *J. Phys. Chem. B* **1999**, *103*, 7122.
(32) Hait, S. K.; Moulik, S. P.; Rodgers, M. P.; Burke, S. E.; Palepu, R. *J. Phys. Chem. B* **2001**, *105*, 7145.
(33) Alexandridis, P.; Holzwarth, J. F.; Hatton, T. A. *J. Phys. Chem.* **1995**, *99*, 8222.
(34) Koper, G. J. M.; Sager, W. F. C.; Smeets, J.; Bedeaux, D. *J. Phys. Chem.* **1995**, *99*, 13291.
(35) Eicke, H. F.; Meier, W.; Hammerich, H. *Colloids Surf., A* **1996**, *118*, 141.
(36) Eicke, H. F.; Thomas, H. *Langmuir* **1999**, *15*, 400.
(37) Eicke, H. F. *J. Phys. Chem. B* **2001**, *105*, 2753.
(38) Mays, H. *J. Phys. Chem. B* **1997**, *101*, 10271.
(39) Liu, D.; Ma, J.; Cheng, H.; Zhao, Z. *J. Dispersion Sci. Technol.* **1999**, *20*, 513.
(40) Mukhopadhyay, L.; Bhattacharya, P. K.; Moulik, S. P. *Colloids Surf.* **1990**, *50*, 295.
(41) Perez-Casas, S.; Castillo, R.; Costas, M. *J. Phys. Chem. B* **1997**, *101*, 7043.
(42) Hamilton, R. T.; Billman, J. F.; Kaler, E. W. *Langmuir* **1990**, *6*, 1696.
(43) Mays, H.; Ilgenfritz, G. *J. Chem. Soc., Faraday Trans.* **1996**, *92*, 3145.
(44) Rharbi, Y.; Li, M.; Winnik, M. A.; Hahn, K. G., Jr. *J. Am. Chem. Soc.* **2000**, *122*, 6242.
(45) Hasegawa, S.; Yamasaki, Y.; Sonta, N.; Shindo, Y.; Sugimura, T.; Kitahara, A. *J. Phys. Chem.* **1996**, *100*, 15575.
(46) Bohne, C.; Abuin, E. B.; Scaiano, J. C. *Langmuir* **1992**, *8*, 469.
(47) Kataoka, H.; Eguchi, T.; Masui, H.; Miyakubo, K.; Nakayama, H.; Nakamura, N. *J. Phys. Chem. B* **2003**,*107*, 12542.
(48) Gebicki, J. L.; Gebicka, L. *J. Phys. Chem. B* **1997**, *101*, 10828.
(49) Mori, Y.; Shinoda, H.; Nakano, T.; Kitagawa, T. *J. Phys. Chem. A* **2002**, *106*, 11743.
(50) Mori, Y.; Shinoda, H.; Nakano, T.; Kitagawa, T. *J. Phys. Chem. A* **2002**, *106*, 11750.
(51) Mori, Y.; Shinoda, H.; Nakano, T.; Kitagawa, T. *J. Photochem. Photobiol., A* **2003**, *157*, 33.
(52) Politi, M. J.; Brandt, O.; Fendler, J. H. *J. Phys. Chem.* **1985**, *89*, 2345.
(53) Rothenberger, G.; Infelta, P. P.; Grätzel, M. *J. Phys. Chem.* **1981**, *85*, 1850.
(54) (a) Maitra, A. *J. Phys. Chem.* **1984**, *88*, 5122. (b) Eicke, H. F.; Rehak, J. *Helv. Chim. Acta* **1976**, *59*, 2833.
(55) The decay of T−T absorption proceeds very slowly in aqueous solution, as shown in Figures 2 and 3. Therefore, the bimolecular rate constants for TTA involve considerable error.
(56) Infelta, P. P.; Grätzel, M. Thomas, J. K. *J. Phys. Chem.* **1974**, *78*, 190.
(57) Tachiya, M. *Chem. Phys. Lett.* **1975**, *33*, 289.
(58) Jóhannsson, R.; Almgren, M.; Alsins, J. *J. Phys. Chem.* **1991**, *95*, 3819.
(59) Almgren, M.; Jóhannsson, R. *J. Phys. Chem.* **1992**, *96*, 9512.